Acta Cryst. (1984). A40, 241–251

Diffraction by a Finite Crystal: General Laue–Bragg Case – Comparison with Approximate Extinction Theories

BY PIERRE BECKER*

Institut Laue–Langevin, 156X, 38042 Grenoble CEDEX, France

AND FRÉDÉRIC DUNSTETTER†

Centre de Mécanique Ondulatoire du CNRS, 23, rue du Maroc, 75019 Paris, France

(*Received* 31 *January* 1983; *accepted* 19 *September* 1983)

Abstract

After a comparison of Kato's theory of extinction with the conventional energy-transfer coupling model, it is shown that both models can be solved exactly for crystals with planar boundaries. Integrated reflecting power can be obtained analytically for a parallelepipedic crystal, which allows for a comparison with approximate treatments (such as the Becker–Coppens Laue formula or the infinite slab expression). For general geometric conditions, numerical integration may be needed. Respective usefulness of various models is discussed.

Introduction

Let us first discuss two types of difficulties in extinction theory.

1. *Nature of the propagation equations*

The most fundamental question is to find a physically meaningful model to describe the propagation of the incident and diffracted beams.

The usual phenomenological model relies on the Zachariasen–Hamilton intensity coupling equations. Let s_0 and s_h be the coordinates along the incident-beam direction (intensity I_0) and the diffracted beam direction (intensity I_h). The coupling equations are

$$\frac{\partial I_0}{\partial s_0} = -\sigma I_0 + \sigma I_h$$
$$\frac{\partial I_h}{\partial s_h} = -\sigma I_h + \sigma I_0. \qquad (1)$$

Absorption is neglected here (see Becker & Coppens, 1974). The model assumes a wide homogeneous incident beam described by plane waves, and therefore the coupling term σ, as well as I_0 and I_h, are functions of the divergence ε of the incident beam. $\sigma(\varepsilon)$ represents the effective kinematical cross section of the distorted crystal and verifies

$$\int \sigma(\varepsilon)\, \mathrm{d}\varepsilon = Q, \qquad (2)$$

where Q, the kinematical total cross section per unit volume, is

$$Q = \left|\frac{CF}{V}\right|^2 \frac{\lambda^3}{\sin 2\theta}, \qquad (3)$$

with C = polarization factor $\times r_e$ for photons, $C = 10^{-12}$ cm for neutrons, F is the structure factor and V denotes the unit-cell volume. The crystal volume being v, for an incident beam of unit intensity, the kinematical power is

$$\mathcal{P}_k = vQ. \qquad (4)$$

This model has been widely used, and has proved to be very successful in reproducing experimental trends even in cases of severe extinction. However, drawbacks are well known, especially due to the strong dependence on the shape of the function σ and the physical meaning of its line width.

More recently, starting from Takagi's equations, Kato (1976, 1979) has shown that one may write intensity coupling equations under very definite conditions. Kato defines a phase correlation function $f(\mathbf{t}) = \langle \exp[2i\mathbf{H}\,.\,\mathbf{u}(\mathbf{r})] \exp[-2\pi i\mathbf{H}\,.\,\mathbf{u}(\mathbf{r}+\mathbf{t})]\rangle$, where $\mathbf{H}$ is the Bragg vector and $\mathbf{u}(\mathbf{r})$ is the local distorsion vector. Defining τ as being a characteristic width of $f(\mathbf{t})$ (correlation distance) and remembering the definition of the critical dynamical dimension Λ (extinction distance in a symmetrical case)

$$\Lambda = \left\{\frac{Q \sin 2\theta}{\lambda}\right\}^{-1/2} = \frac{V}{\lambda C|F|}. \qquad (5)$$

Kato has explicitly shown that if

$$\tau \ll \Lambda \qquad (6)$$

equations (1) are still valid. However, his derivation

* On leave of absence from Laboratoire de Cristallographie, Université de Nancy I, BP 239, 54506 Vandoeuvre CEDEX, France.

† Present address: Laboratoire Léon Brillouin, CEN Saclay, 91191 Gif-sur-Yvette CEDEX, France.

0108-7673/84/030241-11$01.50

originates from a spherical wave description. Hence, the coupling term σ (which we will denote by σ^K) is a constant:

$$\sigma^K = 2\tau/\Lambda^2. \tag{7}$$

(We will write, for this model, the intensity as I_0^K and I_h^K.) Kato has proposed corrections to be applied when $\tau \sim \Lambda$, where primary extinction becomes important.

It is very clear that by reducing the wavelength one increases the chance for (1) to be valid.

It occurs in practice that the conventional model is better adapted to experimental situations than Kato's simple model. We believe that this is due to (6) being rarely satisfied, which means that 'real crystals' may be often more perfect than we expect. We also believe that one of the reasons for the success of conventional models comes from the fact that, for severe extinction, the solution has an asymptotic limit similar to a dynamical behaviour ($P \propto |F|$).

We would like to end this discussion by pointing out the most recent general statistical approach of Kato (1980*b*, 1982), which in principle covers the whole range between perfect and ideally imperfect crystals. This theory separates the coherent from the incoherent part of the beams and results in two sets of dependent propagation equations. The model is therefore very complex for a general crystal geometry but it is rather urgent to solve, even approximately, this attractive approach. Kato so far has produced a solution only for symmetrical Laue geometry in an infinite parallel slab.

In the present paper, we shall assume that (1) [or modified by (6)] are a valid approximation.

2. *Nature of the solution*

There exists a second difficulty, connected with the boundary conditions at the surface of the crystal. It has been shown (Becker & Coppens, 1974; Bonnet, Delapalme, Becker & Fuess, 1976) that a general solution of (1) is easy to get in a pure Laue geometry, when the entrance surface of the incident beam does not overlap with the exit surface of the scattered beam. A general configuration is sketched in Fig. 1.

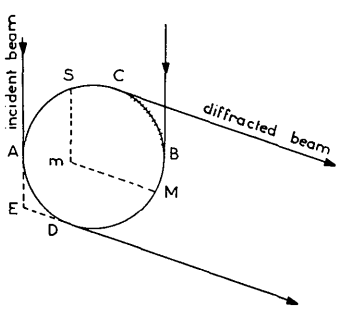

Fig. 1. General diffraction configuration, showing the ambiguity in the boundary conditions on the portion *BC*.

It is easily seen that no simple boundary condition can be written for the portion $\widehat{CB}$ which is in a reflexion (Bragg) situation. The smaller the Bragg angle θ, the less important the ambiguity: another advantage of using small wavelengths.

The approximate solution of Becker & Coppens (1974), which has been used for a general crystal shape, and led to a programmable expression for extinction, consists in neglecting the corrections due to the portion $\widehat{CB}$, and therefore in locally using the Laue-case solution.

It is in fact the purpose of the present paper to show that a general analytical solution to equations of type (1) is possible for a mixed Laue–Bragg configuration. We shall consider explicitly a crystal in the shape of a parallelepiped. It will therefore be possible to discuss the conventional model *versus* Kato's model. It will also be of great interest to discuss the validity of the Becker–Coppens approximation, and also to see under what conditions we can approximate a finite plate by an infinite slab.

Calculations of wavefields for mixed Laue–Bragg geometries have already been considered by Saka, Katagawa & Kato (1972) who obtained the expression for wave amplitudes inside a perfect sample.

Geometrical considerations and boundary conditions

In order to solve the boundary conditions for a general situation similar to Fig. 1, we decompose the entrance surface $\widehat{ACB}$ into a superposition of point sources S. If M is a point on the exit part of the surface $\widehat{CBD}$, the pair of points (S, M) uniquely defines a point m which may vary in the extended volume v' defined by the contour $\widehat{ACBMDEA}$ (see Becker, 1977). If we call $I(m)$ the intensity at M coming from the point source S: $I(m) = I_h(S \rightarrow M)$, the diffracted power is given by

$$P = \int_{v'} I(m)\, \mathrm{d}v_m. \tag{8}$$

Conventional treatments involve a further integration over ε, leading to

$$\mathscr{P} = \int P\, \mathrm{d}\varepsilon. \tag{8'}$$

In Kato's approach

$$\mathscr{P}^K = \frac{\lambda}{\sin 2\theta} \int_{v'} I^K(m)\, \mathrm{d}v_m. \tag{9}$$

With the point sources, the boundary conditions are very simple. On the entrance surface:

$$I_0 = \delta(s_h). \tag{10}$$

Let us make the following transformation:

$$\begin{aligned} I_0 &= J_0 \exp[-\sigma(s_0 + s_h)] \\ I_h &= J_h \exp[-\sigma(s_0 + s_h)]. \end{aligned} \tag{11}$$

Equations (1) become the system

$$\frac{\partial J_0}{\partial s_0} = \sigma J_h$$
$$\frac{\partial J_h}{\partial s_h} = \sigma J_0 \qquad (12)$$

(and similar for Kato's theory).

In the conventional treatment, we have shown (Becker, 1977) that

$$\lim_{\eta \to 0} J_h(s_0, \eta) = \sigma. \qquad (13)$$

However, in Kato's theory, the same condition cannot apply, since τ involves multiple scattering. Kato (1980*a*) has shown that

$$\lim_{\eta \to 0} J_h^K(s_0, \eta) = 1/\Lambda^2. \qquad (13')$$

Generally we may write

$$I_h^K(m) = \frac{1}{2\tau} I_h(m, \sigma^K). \qquad (14)$$

We now consider the possible scattering geometries of diffraction for a rectangular crystal (Fig. 2). In the case of Fig. 2(*a*), there is no overlap between entrance and exit surfaces. This is the pure 'Laue geometry' which was dealt with previously (Bonnet *et al.*, 1976). Fig. 2(*c*), corresponds to the pure reflexion case. It is clear that the Bragg angle θ is large in this case, so that extinction is very small. We therefore discard this configuration.

We shall here explicitly consider the configuration of Fig. 2(*b*), corresponding to an intermediate case, where the entrance and exit surfaces partly overlap (*AB*). Extended volumes v' corresponding to possible points m are shown in Fig. 3. Restricting ourselves now to case (*b*), we can distinguish between four distinct configurations for point m, represented in Fig. 4. For multiple scattering processes, all points within the shaded domains can be excited as local scattering sites. Notice, however, that case (4) can only be encountered in the case of a flat crystal or for a large Bragg angle: in the following, we shall discard such a case. Let us denote the dimensions of the sample as

$$a = AB = CD$$
$$b = BC = DA.$$

We shall not encounter the situation of Fig. 4(*a*) as long as

$$\tan \alpha_0 < b/a, \tan \alpha_h < b/a, \qquad (15)$$

the angles α_0 and α_h being defined in Fig. 2. Thus, for each point m inside v' (Fig. 2*b*), we calculate $I(m)$ and then integrate through (8) or (9). v' can be divided into three domains, according to the configuration for point m (Fig. 5) where the subdivision of domain 2 will appear later.

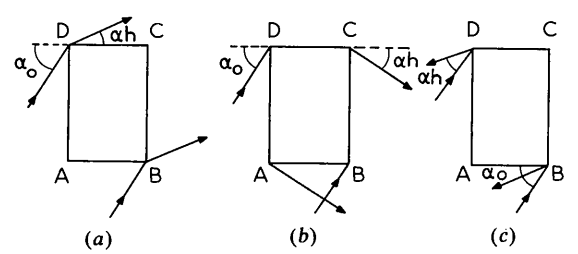

Fig. 2. Scattering geometries for a rectangular crystal. (*a*) Transmission, (*b*) mixed case, (*c*) reflexion.

Calculation of intensity coming from a point source

1. If m belongs to domain 1, the solution is that calculated by Becker (1977):

$$J_1(m) = \sigma I_0[2\sigma(s_0 s_h)^{1/2}], \qquad (16)$$

where $s_0 = \overline{sm}$, $s_h = \overline{mM}$ (Fig. 4) and I_0 is a modified Bessel function.

2. Suppose now that m belongs to domain 2. Four cases, each corresponding to a subdomain of Fig. 5, are represented in Fig. 6. The four cases can be treated uniquely, defining the main parameter

$$c = \overline{SH}$$

(which can be zero).

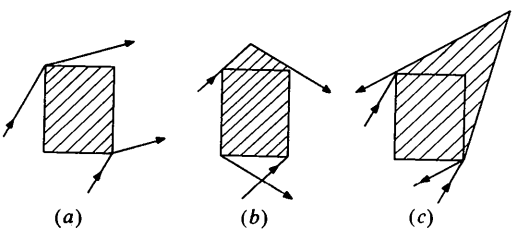

Fig. 3. Extended volume v' where point m can vary.

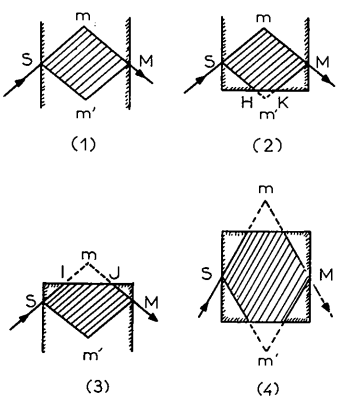

Fig. 4. The four distinct situations for the point m with respect to crystal boundary. Case (4) will be discarded in this paper.

Let P (coordinates u, v) be a current point in the shaded area with respect to the origin S. We must distinguish the two situations

$$v < c \ (P^-)$$
$$v > c \ (P^+).$$

Crystal boundary AB is defined by the equation

$$v - c = \frac{\beta_0}{\beta_h} u \tag{17}$$

with

$$\beta_0 = \sin \alpha_0, \ \beta_h = \sin \alpha_h.$$

Let J_0^-, J_h^- be the solution of (12) for a point P^-, and J_0^+, J_h^+ the solution for a point P^+. M is of P^+ type. The solution of (12) can formally be written

$$J_h^+(s_0, s_h) = \sigma^2 \int_0^c dv \int_0^{s_0} du \, J_h^-(u, v) + \sigma^2 \int_c^{s_h} dv \int_{(\beta_h/\beta_0)(v-c)}^{s_0} du \, J_h^+(u, v) + \sigma. \tag{18}$$

J_h^- is given by (16).

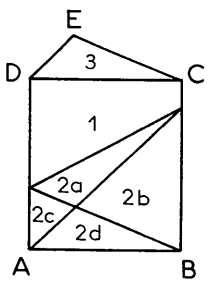

Fig. 5. Subdivision of volume v', according to situation for m depicted in Fig. 4.

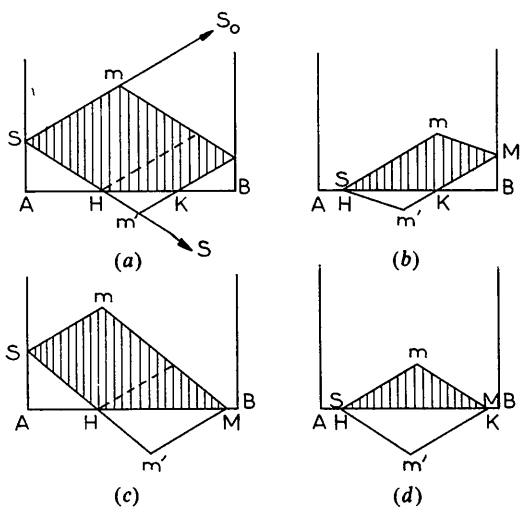

Fig. 6. Geometric construction for domain 2, in the calculation of $I(m)$.

We can formally write (18) as

$$(1 - \hat{L}) J_h = \sigma, \tag{19}$$

which is inverted into

$$J_h = \sum_{n=0}^{\infty} \hat{L}^n(\sigma) = \sum_{n=0}^{\infty} a_n \sigma^{2n+1}. \tag{20}$$

We get immediately

$$a_0 = 1$$

$$\begin{cases} a_1 = a_1^- = s_0 s_h & (s_h < c) \\ a_1 = a_1^+ = s_0 s_h - (\beta_h/\beta_0)\frac{1}{2}(s_h - c)^2 & (s_h > c) \end{cases}$$

$$\begin{cases} a_n^- = s_0^n s_h^n / n!\, n! \\ a_n^+ = (s_0^n s_h^n / n!\, n!) - (\beta_h/\beta_0) \\ \qquad \times \dfrac{[(s_h - c)^{n+1}(s_0 + \beta_h/\beta_0 c)^{n-1}]}{[(n+1)!(n-1)!]^{-1}}. \end{cases}$$

The final result is

$$J_2(m) = J_h^+(s_0, s_h) = \sigma \left\{ I_0[2\sigma(s_0 s_h)^{1/2}] - \frac{\beta_h}{\beta_0} \frac{(s_h - c)}{[s_0 + (\beta_h/\beta_0)c]} \times I_2(2\sigma\{(s_h - c)[s_0 + (\beta_h/\beta_0)c]\}^{1/2}) \right\}. \tag{21}$$

3. When m belongs to domain 3, the situation is represented in Fig. 7. M cannot be reached from S through a single scattering. The lowest-order term in J_h must be $0(\sigma^3)$. We shall consider the solution for J_0 rather than for J_h. We denote $c = \overline{SI}$. The boundary (CD) obeys the equation

$$V = (\beta_0/\beta_h)(u - c) \tag{22}$$

and

$$\begin{aligned} J_h(s_0, 0) &= \sigma & (s_0 < c) \\ J_h[s_0, (\beta_0/\beta_h)(s_0 - c)] &= 0 & (s_0 > c). \end{aligned} \tag{22'}$$

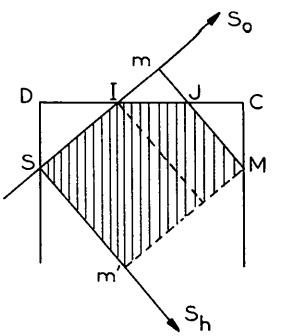

Fig. 7. Geometric construction for domain 3.

As in case (2), we distinguish P^- ($s_0 < c$) from P^+ ($s_0 > c$) and through similar arguments we show that

$$J_3(m) = J_h^+(s_0, s_h) = \sigma\{I_0[2\sigma(s_0 s_h)^{+1/2}] - I_0[2\sigma\{(s_0 - c)[s_h + (\beta_0/\beta_h)c]\}]^{1/2}\}. \quad (23)$$

4. Integration: we shall denote by m, m_2, m_3 the points m in the three domains 1, 2, 3. The approximate Becker–Coppens (BC) solution, used in the general program *LINEX*, is

$$J_h^{BC} = J_1(m)$$

given by (16). We see that actual intensities are smaller than J^{BC} for points m_2 or m_3. However, the volume v' is larger than in the BC approximation where

$$\mathcal{P}^{BC} = \int_v I_h^{BC}(m)\, dv_m.$$

There is a partial compensation of the error in the approximate solution.

5. Expressions such as $J_1(m)$, $J_2(m)$, $J_3(m)$ can be used very generally in numerically estimating the integrated power, and that for general shapes of crystals. In Fig. 8, we show how they can be employed to get better estimates than the BC approximation. For m_1, J_1 can be applied. For m_2 (m_3), J_2 (J_3) have to be used, provided the curvilinear segments limiting shaded domains are replaced by straight lines.

Kato (1982) has developed a similar scheme for a sphere and Dunstetter (1981) also proposed a solution for a perfect sample.

In the following, we want an accurate comparison of various approaches and we show that extinction can be obtained analytically for a symmetrical geometry ($\alpha_0 = \alpha_h = \theta$). We therefore derive this exact solution.

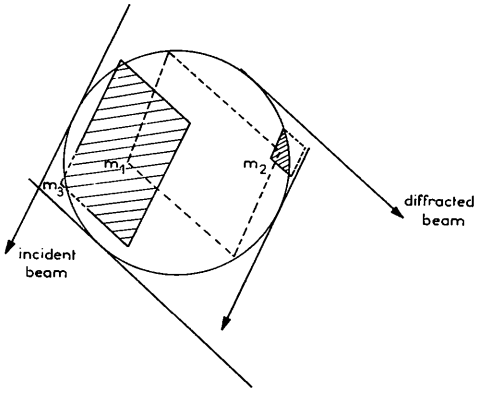

Fig. 8. Possible scattering configuration for a crystal of general shape.

Diffracted power for symmetrical case

Diffracted power $\mathcal{P}$ per unit height of the crystal along z (equation 8) is written as

$$\mathcal{P} = \mathcal{P}_K \varphi, \quad (24)$$

where $\mathcal{P}_k = \sigma ab$ in conventional models, $\mathcal{P}_k^K = Q ab$ in Kato's model.

We sketch once more the geometric conditions for the symmetric case in Fig. 9. We also introduce the following notations:

$$\gamma = \cos\theta \qquad \beta = \sin\theta$$
$$u = \sigma\xi/\gamma \qquad v = \sigma\eta/\beta$$

[for domain 3 $v = \sigma(\eta - b)/\beta$]

$$\rho = (a/b)\tan\theta \qquad x = \sigma a/\gamma. \quad (25)$$

For domain 1 the integration is straightforward

$$\varphi_1 = (1-\rho)\frac{e^{-x}}{x}\int_0^x I_0\{2[u(x-u)]^{1/2}\}\, du.$$

Developing the Bessel function and using expressions of Appendix *A*, we obtain

$$\varphi_1 = (1-\rho)\frac{e^{-x}}{x}\sin hx. \quad (26)$$

When $\rho \to 0$, the solution becomes that of the 'infinite parallel plate':

$$\varphi^\infty = \frac{e^{-x}}{x}\sin hx. \quad (27)$$

From the general expression for $I(m)$ obtained previously, φ can always be written as:

$$\varphi(x, \rho) = \varphi^\infty(x) + \rho\Delta\varphi^{BC}(x).$$

Similarly, the Becker–Coppens approximation is written

$$\varphi^{BC}(x, \rho) = \varphi^\infty(x) + \rho\Delta\varphi^{BC}(x). \quad (28)$$

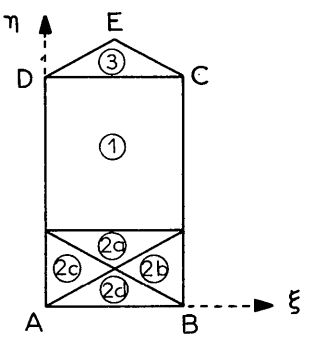

Fig. 9. Domains in the symmetrical case; the integrated power is $P = P_1 + P_2 + P_3$.

Applying the solution found for $I(m)$ in the preceding sections, and introducing the proper changes of variables, we can show that

$$\Delta\varphi^{BC}(x)=\frac{2}{x^2}\int_0^{x/2}du\int_u^{x-u}dv\,e^{-(u+v)}I_0[2(uv)^{1/2}]$$
$$+\frac{2}{x^2}\int_0^{x/2}du\int_0^{u}dv\,e^{-2v}I_0(2v)$$
$$-2\frac{e^{-x}}{x^2}\int_0^{x/2}du\int_0^{x-u}dv\,I_0\{2[u(x-u)]^{1/2}\}; \tag{29}$$

$$\Delta\varphi(x)=\Delta\varphi^{BC}(x)$$
$$+2\frac{e^{-x}}{x^2}\int_0^{x/2}du\int_0^{u}dv\,\{I_0\{2[u(x-u)]^{1/2}\}$$
$$-I_0\{2[v(x-v)]^{1/2}\}\}$$
$$-2\frac{e^{-x}}{x^2}\int_0^{x/2}du\int_{x-u}^{x}dv\,[(x-v)/v]$$
$$\times I_2\{2[v(x-v)]^{1/2}\}$$
$$-\frac{2}{x^2}\int_0^{x/2}du\int_u^{x-u}dv\,e^{-(u+v)}(u/v)I_2[2(uv)^{1/2}]$$
$$-\frac{2}{x^2}\int_0^{x/2}du\int_0^{u}dv\,e^{-2v}I_2(2v). \tag{30}$$

The integrals are evaluated in Appendix *B*, and one finally obtains

$$\Phi(x,\rho)=\frac{e^{-x}}{x}\sin hx$$
$$+\frac{\rho}{x}\left[1-\frac{e^{-x}\sin hx}{x}-2e^{-x}I_1(x)\right] \tag{31}$$

$$\Phi^{BC}(x,\rho)=\frac{e^{-x}}{x}\sin hx+\rho\left\{\frac{1}{2x}-\frac{e^{-x}\sin hx}{2x}\right.$$
$$\left.-\frac{e^{-x}\sin hx}{2x^2}+\frac{e^{-x}}{3}[I_1(x)+I_2(x)]\right\}. \tag{32}$$

Discussion

Discussion of the previous result (31)–(32) is relevant to Kato's model. Φ is the extinction factor in this theory.

One should notice that, generally, the extinction factor is considered as a function of $X=\sigma\bar{T}$, where $\bar{T}$ is the mean path through the crystal. It is straightforward to show that

$$\bar{T}=\frac{a}{\gamma}[1-\rho/3]=\bar{T}_\infty(1-\rho/3). \tag{33}$$

Therefore, if using X rather than x, we have to apply the scaling law:

$$X=(1-\rho/3)x. \tag{33'}$$

The following property is immediately observed:

$$\varphi_\infty<\varphi<\varphi^{BC}.$$

We present the three functions φ_∞, $\Delta\varphi$, $\Delta\varphi^{BC}$ in Fig. 10, and the extinction factors φ_∞, φ, φ^{BC} are shown for $\rho=1$ in Fig. 11. It is observed that, even for reasonable extinction ($\varphi\sim0.5$), the correction to the Becker–Coppens approximation is highly significant. The deviation from the infinite-slab approximation is also quite marked. To see this point more precisely, we plot

$$\chi_1=\frac{\varphi-\varphi^\infty}{\varphi},\qquad \chi_2=\frac{\varphi^{BC}-\varphi}{\varphi} \tag{34}$$

as a function of x, for various values of ρ (Fig. 12).

For small values of x, a Taylor expansion shows that, to first order

$$\varphi^\infty\sim1-x$$
$$\varphi\sim\varphi^{BC}\sim1-x \tag{35}$$

as expected from general arguments (Becker & Coppens, 1974).

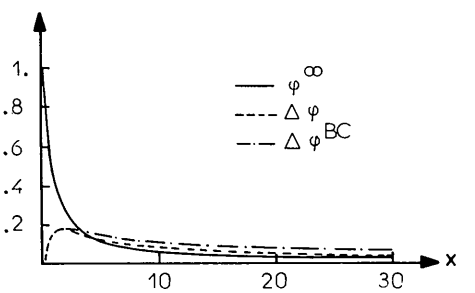

Fig. 10. Contributions to the extinction factor φ, as appearing in the text.

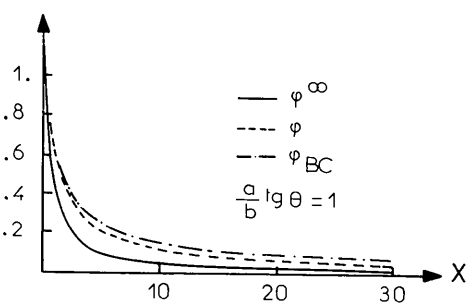

Fig. 11. Various approximations for φ when $\rho=1$.

The limit for strong x is interesting to look at. Using the result

$$\lim_{t\to\infty} e^{-t} I_n(t) = 1/(2\pi t)^{1/2}$$

we find

$$\begin{aligned} \varphi &\sim [1+2\rho](1/2x) \\ \varphi &\sim \frac{2\rho}{3(2\pi)^{1/2}} x^{-1/2}. \end{aligned} \tag{36}$$

Of course, absorption should be included in this limit. However, we observe that $\mathcal{P}_\infty$ or $\mathcal{P}$ tend towards a constant limit, independent of the structure factor: for instance, with $\varphi_\infty \sim 0.5$, $\mathcal{P}_\infty$ is rather insensitive to F. It is well known from practical applications that such behaviour is not adapted to real data for severe extinction. As pointed out by Kato (1980*c*), when $x \sim 1$, $\mathcal{P}_\infty$ is smaller than $\mathcal{P}_{\rm dyn}$ (calculated for a perfect crystal), which is physically nonsense. Φ is the extinction correction in Kato's theory in the incoherent scattering limit $\{\langle \exp[2\pi i \mathbf{H}\,.\,\mathbf{u}(\mathbf{r})]\rangle_{\mathbf{r}} = 0\}$: such a model is only valid when $x < 1$, *i.e.* when $\tau T/\Lambda^2 < 1$.

The Becker–Coppens approximation has a rather different limit for large x, since $P^{\rm BC} \propto |F|$ and thus mimics the dynamical behaviour for strong coupling. This behaviour is an artefact of the approximations introduced, but may be a reason for the success of the method in terms of applications to real situations.

Extinction factor for Darwin–Zachariasen model

In the conventional models, we have seen that the coupling term σ is a function of the angle ε of departure from the Bragg condition. We therefore have to integrate the power P over the angle ε. More precisely, the extinction factor y, defined as $(\mathcal{P}/\mathcal{P}_k)$, is given by

$$y = Q^{-1} \int_{-\infty}^{+\infty} \sigma(\varepsilon)\varphi[\sigma(\varepsilon)a/\gamma]\,d\varepsilon. \tag{37}$$

We shall further assume that σ can be approximated by a Lorentzian:

$$\sigma(\varepsilon) = \frac{2gQ}{1+(\pi g\varepsilon)^2} = \frac{\sigma(0)}{1+(\pi g\varepsilon)^2}. \tag{38}$$

We define the usual extinction parameter

$$x_s = \frac{1}{2}\sigma(0)(a/\gamma) = gQT_\infty, \tag{39}$$

which corresponds to the infinite plate case. As in the description of φ, we may scale T_∞ for a finite crystal and define

$$X_s = gQT = x_s[1-\tfrac{1}{3}\rho]. \tag{39'}$$

A generalization of (28) leads to

$$\begin{aligned} y &= y^\infty + \rho\Delta y \\ y^{\rm BC} &= y^\infty + \rho\Delta y^{\rm BC}. \end{aligned} \tag{40}$$

y^∞ was calculated by Bonnet *et al.* (1976):

$$y^\infty = e^{-2x_s}\{I_0(2x_s) + I_1(2x_s)\}. \tag{41}$$

The terms Δy and $\Delta y^{\rm BC}$ are calculable (Appendix *C*) and are given by

$$\begin{aligned} \Delta y &= \frac{4}{3}y^\infty - \frac{1}{3x_s}e^{-2x_s}I_1(2x_s) \\ &\quad -[1+{}_2F_2(\tfrac{1}{2},\tfrac{3}{2};1,3;-4x_s)] \\ \Delta y^{\rm BC} &= \frac{1}{6}\left[y^\infty - \frac{1}{x_s}e^{-2x_s}I_1(2x_s)\right] \\ &\quad + \frac{x_s}{6}[1+{}_2F_2(\tfrac{3}{2},\tfrac{3}{2};2,4;-4x_s)], \end{aligned} \tag{42}$$

where ${}_2F_2$ is a generalized hypergeometric function. The characteristics of (40) are summarized in Figs. 13 and 14, and the conclusions are similar to those relative to φ. In particular, for a given x_s,

$$y^\infty < y < y^{\rm BC}; \tag{43}$$

when x_s is small

$$\begin{aligned} y^\infty &\sim 1 - x_s \\ y \sim y^{\rm BC} &\sim 1 - x_s. \end{aligned} \tag{44}$$

In the case of strong extinction, the following asymptotic behaviour is observed:

$$y^\infty \sim \frac{1}{[\pi x_s]^{1/2}}.$$

The function ${}_2F_2$ has to be calculated numerically

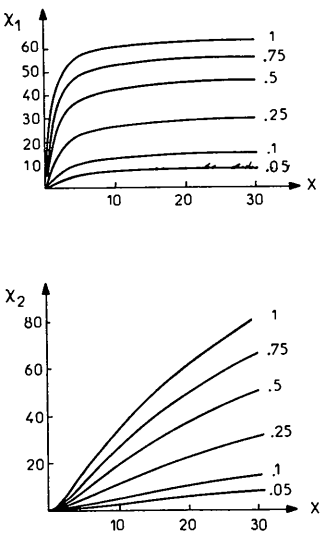

Fig. 12. Relative variation of the extinction factor as a function of the parameter x, for different values of ρ.

and one observes

$$y^{\infty} \sim \left[1+\frac{\rho}{2}\right]\frac{1}{[\pi x_s]^{1/2}}, \qquad (45)$$

so that for strong reflections and severe extinction, the integrated power becomes proportional to $|F|$, and remains in the range $\mathcal{P}_{dyn}$, $\mathcal{P}_{kin}$. This is a fairly major difference with φ (or Kato's extinction factor) and is obviously responsible for the practical success of the conventional treatment of extinction. It should, however, be noted that the most recent formulation of statistical theory of diffraction by Kato (1980*b*, 1982) contains a coherent and an incoherent contribution to the diffracted beam and should in principle overcome this difficulty. It is thus urgent to test this theory. One of us (PB) had a rather extended discussion with Kato about this 'ε dependence problem' in conventional models. One may summarize the discussion as follows: the kinematical cross section $\sigma(\varepsilon)$ broadens the beam as it travels within the crystal: thus, in general, the energy conservation for a given value of the divergence ε should be violated, in contradiction with (1) which is thus too strict a constraint. This important point will be discussed separately.

We may also plot

$$\frac{\Delta y^{\infty}}{y} = \frac{y - y^{\infty}}{y}$$

$$\frac{\Delta y^{BC}}{y} = \frac{y^{BC} - y}{y}$$

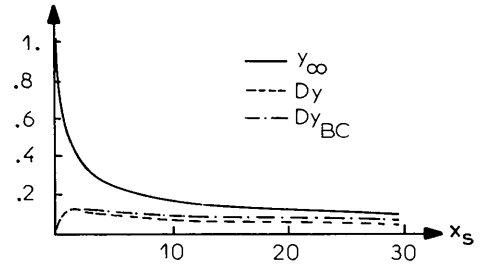

Fig. 13. Contribution to the extinction factor y, as appearing in the text.

(*a*)

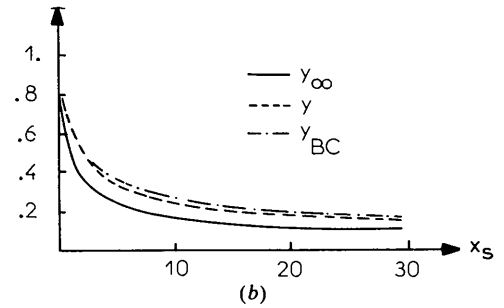

(*b*)

Fig. 14. Approximations for y, where $\rho = 1$.

as a function of x_s for various values of ρ (Fig. 15). Though less marked than for φ, the influence of the finiteness of the crystal is rather important; it appears also that the BC approximation should be reconsidered for cases of severe extinction.

Conclusions

We have shown that, for a crystal with planar boundaries, it is possible to calculate analytically the intensity scattered from a point source. For general geometrical conditions, the diffracted power can be evaluated numerically by integration of these local intensity functions. We have shown that for a parallelepiped, in symmetrical geometry, the diffracted power can be calculated exactly by analytical functions, which allowed us to discuss some approximate solutions, such as the Becker–Coppens approximate-solution least-squares routine and the infinite-slab solution. Corrections to those approximations are important for severe extinction.

We have also discussed the behaviour of the solution to Darwin energy transfer equations, as compared to Kato's formulation of diffraction by statistically distorted crystals (starting from Takagi's dynamical equations). Kato's model in the limit of incoherent beam (energy transfer equations) leads to a formulation similar to Darwin's equations (except for the integration over divergence angle which disappears with Kato, since the theory is based on spherical waves): the behaviour for strong coupling leads to a power that does not depend strongly on the structure factor, though the ε integration gives a dependence on $|F|$. Most crystals behave according to the conventional models in this sense. Dynamical behaviour (coherent beam) is also $|F|$ dependent, so that Kato's complete theory with a progressive build up of incoherence from the defects as the beam travels in the sample should be a physically better solution, though

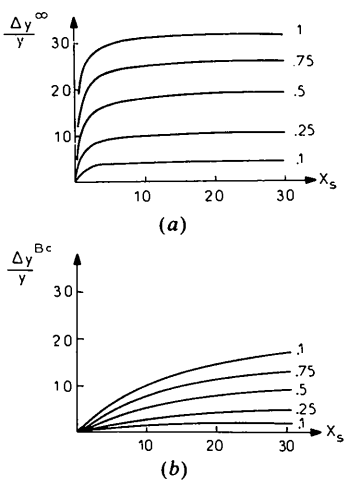

(*a*)

(*b*)

Fig. 15. $\Delta y/y$ and $\Delta y^{BC}/y^{BC}$ as functions of x_s, for various values of ρ.

more difficult. But, even in this complete theory, the framework of the calculation of extinction will remain the same as discussed in this paper.

APPENDIX A

Summary of some useful integrals and expressions (Abramowitz & Stegun, 1965).

1. $$I_n(x)=\left(\frac{x}{2}\right)^n\sum_{k=0}^{\infty}\frac{(x/2)^{2k}}{k!(n+k)!} \tag{A.1}$$

$$e^{-x}I_n(x)=(-1)^n\sum_{k=n}^{\infty}\frac{(-1)^k}{k!}\binom{2k}{k-n}\left(\frac{x}{2}\right)^k. \tag{A.2}$$

2. $$\int_0^x e^{-t}I_0(t)\,dt=x\,e^{-x}[I_0(x)+I_1(x)] \tag{A.3}$$

$$\int_0^x e^{-t}I_1(t)\,dt=x\,e^{-x}[I_0(x)+I_1(x)]+e^{-x}I_0(x)-1. \tag{A.4}$$

For $n\geq 2$

$$\int_0^x e^{-t}I_n(t)\,dt=x\,e^{-x}[I_0(x+I_1(x)]+n[e^{-x}I_0(x)-1]+2\,e^{-x}\sum_{p=1}^{n-1}(n-p)I_p(x) \tag{A.5}$$

$$\int_0^x e^{-t}t^nI_n(t)\,dt=\frac{e^{-x}x^{n+1}}{2n+1}[I_n(x)+I_{n+1}(x)]. \tag{A.6}$$

3. $$\frac{dI_0(x)}{dx}=I_1(x)$$

$$\frac{dI_n}{dx}=I_{n+1}(x)+\frac{n}{x}I_n(x). \tag{A.7}$$

4. $$\int_0^x dt\frac{t^p(x-t)^q}{p!q!}=\frac{x^{p+q+1}}{(p+q+1)!} \tag{A.8}$$

$$\int_0^{x/2} dt\frac{t^p(x-t)^q}{pq}=\left(\frac{x}{2}\right)^{p+q+1}\frac{1}{(p+q+1)!}\sum_{k=0}^{q}\binom{p+q+1}{k} \tag{A.9}$$

$$\int_0^{\alpha} dt\frac{t^n(x-t)^n}{n!n!}=\sum_{p=0}^{n}\frac{\alpha^{n+p+1}(x-\alpha)^{n-p}}{(n+p+1)!(n-p)!}. \tag{A.10}$$

5. $$\sum_{k=0}^{n}\binom{2n+1}{k}=2^{2n} \tag{A.11}$$

$$\sum_{k=0}^{n}\binom{2n+2}{k}=\frac{1}{2}\left\{2^{2n+2}-\binom{2n+1}{n+1}\right\} \tag{A.12}$$

$$\sum_{p=0}^{n}\sum_{k=0}^{n-p}\binom{2n+2}{k}=\sum_{k=0}^{n}(n-k+1)\binom{2n+2}{k}=\frac{1}{2}\frac{(2n+2)!}{n!(n+1)!}. \tag{A.13}$$

6. From (A.11) and (A.12), one can show that

$$\int_0^{x/2}\frac{t^n(x-t)^n}{n!n!}dt=\frac{1}{2}\left(\frac{x}{2}\right)^{2n+1}\frac{1}{(2n+1)!} \tag{A.14}$$

$$\int_0^{x/2}\frac{t^{n+1}(x-t)^n}{(n+1)!n!}dt=\frac{1}{2}\left\{\frac{x^{2n+2}}{(2n+2)!}-\frac{(x/2)^{2n+2}}{(n+1)!(n+1)!}\right\}. \tag{A.15}$$

APPENDIX B

Calculation of the extinction factor $\varphi(x)$

In order to calculate $\varphi(x)$ and $\varphi^{BC}(x)$, some rather difficult integrals have to be evaluated.

(26) is obtained by use of (A.8).

(29) and (30) are derived through simple geometric arguments that will not be reproduced here.

1. We now evaluate

$$B_1=\int_0^{x/2}du\;I_0\{2[u(x-u)]^{1/2}\}$$

$$B_2=\int_0^{x/2}du\,uI_0\{2[u(x-u)]^{1/2}\} \tag{B.1}$$

$$B_3=\int_0^{x/2}du\frac{u}{x-u}I_2\{2[u(x-u)]^{1/2}\}.$$

If Bessel functions are developed (A.1) and if (A.13) and (A.14) are used, we get:

$$B_1=\frac{1}{2}\sinh x$$

$$B_2=\frac{x}{4}[\sinh x-I_1(x)] \tag{B.2}$$

$$B_3=\frac{1}{2}\sinh x-I_1(x).$$

Note that an integration by parts is needed for B_3, in order to use (A.14).

2. Let

$$B_4=\int_0^{x/2} du \int_0^u dv\, I_0\{2[v(x-v)]^{1/2}\}$$
$$B_5=\int_0^{x/2} du \int_{x-u}^{x} dv \frac{x-v}{v} I_2\{2[v(x-v)]^{1/2}\}. \quad (B.3)$$

Using successively (A.1), (A.10), (A.9), (A.13), we get

$$B_4=\frac{x}{4}I_1(x). \quad (B.4)$$

Then, changing $u\to x-u$, $v\to x-v$, and integrating by parts

$$B_5=\frac{x}{4}I_1(x)-\tfrac{1}{2}[\cosh x - I_0(x)]. \quad (B.5)$$

3. We now write

$$B_6=\int_0^{x/2} du \int_u^{x-u} dv\, e^{-(u+v)} I_0[2(uv)^{1/2}]$$
$$B_7=\int_0^{x/2} du \int_u^{x-u} dv\, e^{-(u+v)} \frac{u}{v} I_2[2(uv)^{1/2}]. \quad (B.6)$$

Introducing the new variable $t=u+v$, we write

$$B_6=\int_0^{x} dt\, e^{-t} \int_0^{t/2} du\, I_0\{2[u(t-u)]^{1/2}\}$$
$$B_7=\int_0^{x} dt\, e^{-t} \int_0^{t/2} du \frac{u}{t-u} I_2\{2[u(t-u)]^{1/2}\}.$$

Using (B.2) and (A.4), we obtain

$$B_6=\tfrac{1}{4}[x-e^{-x}\sinh x]$$
$$B_7=B_6-x\,e^{-x}[I_0(x)+I_1(x)]-e^{-x}I_0(x)+1. \quad (B.7)$$

4. Finally we must evaluate

$$B_8=\int_0^{x/2} du \int_0^u dv\, e^{-2v} I_0(2v)$$
$$B_9=\int_0^{x/2} du \int_0^u dv\, e^{-2v} I_2(2v). \quad (B.8)$$

We make use of (A.3) to (A.7) and obtain through an integration by parts of (A.6)

$$B_8=\frac{1}{4}\left[\frac{2x^2 e^{-x}}{3}\{I_1(x)+I_2(x)\}+x\,e^{-x}I_1(x)\right]$$
$$B_9=B_8+x\,e^{-x}[I_0(x)+I_1(x)] - \frac{e^{-x}}{2}[x\,e^{x}-I_0(x)]-\frac{x}{2}. \quad (B.9)$$

5. We summarize the results as

$$\Delta\varphi=\frac{2e^{-x}}{x^2}[2B_2-xB_1-B_4-B_5] + \frac{2}{x^2}[B_6-B_7+B_8-B_9] \quad (B.10)$$

$$\Delta\varphi^{BC}=\frac{2e^{-x}}{x^2}[B_2-xB_1]+\frac{2}{x^2}[B_6+B_8]. \quad (B.11)$$

APPENDIX C

Calculation of $y(x_s)$

Let us consider the following expressions:

$$\psi_0=\frac{e^{-x}\sinh x}{x}=\sum_{n=1}^{\infty}\frac{(-2x)^n}{(n+1)!}$$
$$\psi_1=\frac{1}{x}-\frac{e^{-x}\sinh x}{x}=2\sum_{n=0}^{\infty}\frac{(-2x)^n}{(n+2)!}$$
$$\psi_2=\frac{2e^{-x}I_1(x)}{x}=\sum_{n=0}^{\infty}\frac{\binom{2n+2}{n}}{(n+1)!}\left(\frac{-x}{2}\right)^n \quad (C.1)$$
$$\psi_3=\frac{e^{-x}}{3}[I_1(x)+I_2(x)]$$
$$=-\sum_{n=1}^{\infty}\frac{\binom{2n}{n+1}}{n!(n+2)}\left(-\frac{x}{2}\right)^n.$$

It is easy to see that

$$\Delta\varphi=\psi_1-\psi_2$$
$$\Delta\varphi^{BC}=\tfrac{1}{2}[\psi_1-\psi_0]+\psi_3. \quad (C.2)$$

We use the identity

$$\frac{1}{\pi}\int_{-\infty}^{+\infty}\frac{d\eta}{(1+\eta^2)^{n+1}}=2^{-2n}\binom{2n}{n} \quad (C.3)$$

and we define

$$y_\alpha=\frac{1}{\pi}\int_{-\infty}^{+\infty}\psi_\alpha\left[\frac{2x_s}{1+\eta^2}\right]\frac{d\eta}{1+\eta^2} \quad (C.4)$$

with $\alpha=0, 1, 2, 3$.

Therefore

$$y_0=\sum_{n=0}^{\infty}\frac{\binom{2n}{n}}{(n+1)!}(-x_s)^n$$
$$y_1=2\sum_{n=0}^{\infty}\frac{\binom{2n}{n}}{(n+2)!}(-x_s)^n$$
$$y_2=\sum_{n=0}^{\infty}\frac{\binom{2n+2}{n}\binom{2n}{n}}{(n+1)!}\left(\frac{-x_s}{4}\right)^n \quad (C.5)$$
$$y_3=\sum_{n=1}^{\infty}\binom{2n}{n+1}\binom{2n}{n}\left(\frac{-x_s}{4}\right)^n\frac{1}{(n+2)n!}.$$

Table 1. y_2 *and* y_3 *as functions of* x_s

x_s	y_2	y_3	x_s	y_2	y_3
0	1	0	3	0·2938	0·0806
0·05	0·9521	0·0079	4	0·2526	0·0794
0·1	0·9086	0·0150	5	0·2246	0·0776
0·2	0·8323	0·0269	6	0·2040	0·0758
0·3	0·7680	0·0366	7	0·1882	0·0740
0·4	0·7133	0·0445	8	0·1755	0·0723
0·5	0·6664	0·0509	9	0·1650	0·0707
0·6	0·6258	0·0561	10	0·1562	0·0692
0·7	0·5906	0·0604	20	0·1091	0·0588
0·8	0·5598	0·0640	30	0·0887	0·0526
0·9	0·5325	0·0670	40	0·0766	0·0484
1	0·5084	0·0694	50	0·0684	0·0452
2	0·3628	0·0797			

These expressions can also be written as

$$y_0 = y^\infty = \frac{1}{2x_s}\int_0^{2x_s} e^{-u} I_0(u)\,du$$

$$y_1 = \frac{1}{2x_s}\int_0^{2x_s} du \int_0^{u} e^{-v} I_0(v)\,dv.$$

From Appendix *B* and the identity,

$$I_2(x) = I_0(x) - \frac{2}{x} I_1(x),$$

$$y_0 = y^\infty = e^{-2x_s}[I_0(2x_s) + I_1(2x_s)] \qquad (C.6)$$

$$y_1 = \frac{4}{3} y_0 - \frac{1}{3x_s} e^{-2x_s} I_1(2x_s). \qquad (C.7)$$

Finally, let the ${}_qF_q$ generalized hypergeometric series be

$${}_pF_q(a_1, \ldots, a_p; b_1, \ldots, b_q; z) = \sum_{n=1}^{\infty} \frac{(a_1)_n \ldots (a_p)_n}{(b_1)_n \ldots (b_q)_n} \frac{z^n}{n!} \qquad (C.8)$$

with $(a)_n = \Gamma(a+n)/\Gamma(a)$.

Then, it follows that

$$y_2 = 1 + {}_2F_2[\tfrac{1}{2}, \tfrac{3}{2}; 1, 3; -4x_s]$$
$$y_3 = \frac{x_s}{6}\{1 + {}_2F_2[\tfrac{3}{2}, \tfrac{3}{2}; 2, 4; -4x_s]\}. \qquad (C.9)$$

y_2 and y_3 are given as functions of x_s in Table 1.

References

ABRAMOWITZ, M. & STEGUN, A. (1965). *Handbook of Mathematical Functions.* New York: Dover.

BECKER, P. (1977). *Acta Cryst.* A**33**, 667–671.

BECKER, P. & COPPENS, P. (1974). *Acta Cryst.* A**30**, 129–147.

BONNET, M., DELAPALME, A., BECKER, P. & FUESS, H. (1976). *Acta Cryst.* A**32**, 945–953.

DUNSTETTER, F. (1981). Thèse de 3ème cycle, Paris.

KATO, N. (1976). *Acta Cryst.* A**32**, 453–466.

KATO, N. (1979). *Acta Cryst.* A**35**, 9–16.

KATO, N. (1980*a*). *Acta Cryst.* A**36**, 171–177.

KATO, N. (1980*b*). *Acta Cryst.* A**36**, 763–778.

KATO, N. (1980*c*). In *Electron and Magnetization Densities in Molecules and Crystals*, edited by P. BECKER. New York: Plenum.

KATO, N. (1982). Sagamore VII Conference Abstracts.

SAKA, T., KATAGAWA, T. & KATO, N. (1972). *Acta Cryst.* A**29**, 192–200.

Acta Cryst. (1984). A**40**, 251–254

Resolution Revisited: Limit of Detail in Electron Density Maps

BY RONALD E. STENKAMP AND LYLE H. JENSEN

Department of Biological Structure and Department of Biochemistry, University of Washington, School of Medicine, Seattle, WA 98195, *USA*

(*Received* 2 *September* 1983; *accepted* 7 *November* 1983)

Abstract

Application of the Rayleigh criterion for the limit of resolution of a simple lens with axial illumination leads to the value 0·61λ. In two-dimensional electron density maps based on X-ray data, the limit of resolution has been considered to be 0·61 d_{min}, the counterpart of the optical case, and in three-dimensional maps 0·715 d_{min}. It is shown here that point atoms separated by these distances are not resolved in two- and three-dimensional electron density maps. Such maps are amplitude functions rather than intensity functions as in the optical case. Application of the Rayleigh criterion to the three-dimensional amplitude function for point atoms leads to a value of 0·917 d_{min} for the limit of resolution in three-dimensional electron density maps. This result is confirmed by superposing both analytic and numeric functions for point atoms and numeric functions for real atoms with $B = 0$ and 10 Å^2. Finally, some implications of diffraction effects in X-ray structure analysis are considered.

In refining models for the met and azidomet forms of hemerythrin, we were particularly interested in the

0108-7673/84/030251-04$01.50